American Mineralogist, Volume 83, pages 835–840, 1998

The hydrous component in andradite garnet

GEORG AMTHAUER* AND GEORGE R. ROSSMAN†

Division of Geological and Planetary Sciences, California Institute of Technology, Pasadena, California 91125, U.S.A.

ABSTRACT

Twenty-two andradite samples from a variety of geological environments and two synthetic hydroandradite samples were studied by Fourier transform IR spectroscopy. Their spectra show that H enters andradite in the form of OH^-. Amounts up to 6 wt% H_2O occur in these samples; those from low-temperature formations contain the most OH^-. Some features in the absorption spectra indicate the hydrogarnet substitution $(SiO_4)^{4-} \leftrightarrow (O_4H_4)^{4-}$ whereas others indicate additional types of OH^- incorporation. The complexity of the spectra due to multi-site distribution of OH^- increases with increasing complexity of the garnet composition.

INTRODUCTION

Systematic studies have shown that hydroxide is a common minor component of grossular and pyrope-almandine-spessartite garnets (Aines and Rossman 1985; Rossman and Aines 1991). Comparable surveys of andradite garnet have not been previously presented. Several reports indicate that appreciable amounts of OH^- can be incorporated in both natural and synthetic andradite-rich garnet (Flint et al. 1941; Peters 1965; Gustafson 1974; Suwa et al. 1976; Onuki et al. 1982; Huckenholz and Fehr 1982; Marcke de Lummen 1986; Kobayashi and Shoji 1987; Kühberger et al. 1989; Wise and Moller 1990; Armbruster and Geiger 1993; Armbruster 1995). Furthermore, elevated OH^- contents have been reported in other Fe^{3+}-rich garnets such as melanite (Lager et al. 1989) and schorlomite (Locock et al. 1995), which suggests that H incorporation in Ca-Fe^{3+} garnet may be a general phenomenon. Solid-solution relationships between andradite, $Ca_3Fe_2(SiO_4)_3$, and hydroandradite, $Ca_3Fe_2(OH)_{12}$, are now established experimentally, and the amount of the hydroandradite component in andradite may be used as geothermometer (Huckenholz and Fehr 1982).

Only a few of these studies provide direct evidence of structural OH^- in andradites by spectroscopic or diffraction methods. Kobayashi and Shoji (1987) report IR spectra of some synthetic andradite-hydroandradite solid solutions. Locock et al. (1995) report an absorption band due to OH^- at 3564 cm^{-1} in the IR spectrum of the Ice River schorlomite with 0.036 wt% H_2O^+. In a crystallographic study, Lager et al. (1989) were unable to locate the H in an andradite (melanite variety) with up to 14% of the Si sites empty. In such H-rich garnets, OH^- most probably occupies tetrahedral sites whereby charge balance is achieved by the well-known hydrogarnet substitution $(O_4H_4)^{4-} \leftrightarrow (SiO_4)^{4-}$. This observation has been confirmed by XRD of a hydrous andradite with a Si deficiency of about 50%, and a high OH content (Armbruster 1995). The structure of this particular sample with space group *Ia3d* is composed of disordered microdomains containing (SiO_4) and (O_4H_4) tetrahedral units.

The aim of the present investigation was to perform a Fourier transform infrared (FTIR) study on different samples of andradite (including Ti-rich melanite) from various geological environments, i.e., different pressures and temperatures of formation, to determine (1) if various types of structural incorporation of OH^- occurs in andradite as in other natural garnets or if there is only the hydrogarnet substitution; (2) the amount of OH that is incorporated in natural andradites; (3) if a correlation exists between the chemical composition and the complexity of the spectra; and (4) the pressure and temperature dependence of OH^- incorporation. Finally, (5) we compare spectroscopic properties of OH^- in natural garnets to those in synthetic hydroandradite.

EXPERIMENTAL METHODS

Samples were obtained mainly from museums. Details of samples, localities, and geological environments are presented in Table 1.

The IR spectra of the natural crystals were recorded from doubly polished single crystals with almost parallel surfaces. The thicknesses of the platelets were between 11.5 and 1185 μm. Measurements were made on clear and inclusion-free as well as crack-free areas of the crystals. In those crystals where color zonation was present, spectra were taken from a selected number of relatively homogeneous parts of the crystal. IR spectra were measured from 114 μm × 114 μm areas using a Nicolet 60SX-FTIR spectrometer equipped with the NicPlan IR microscope and an HgCdTe detector (Rossman and Aines 1991). A 15× reflecting objective and a 10× condenser were used for the measurements. A resolution of 2 cm^{-1}

* Permanent address: Institut für Mineralogie, Universität Salzburg, Hellbrunnerstrasse 34, A-5020 Salzburg, Austria.

† E-mail: grr@gps.caltech.edu

TABLE 1. Andradite samples and their chemical compositions

Sample	Locality	Geology	Variety	Color
GRR1669	Bombay, India	cavity in basalt	hydroandradite	yellow
GA33	Wurlitz, Bavaria, FRG	serpentinite	andradite	yellow-green
GA34	Banat, Romania	serpentinite	andradite	yellow-green
GRR48 rim	Val Malenco, Italy	serpentinite	andradite	yellow-green
GRR134	Val Malenco, Italy	serpentinite	andradite	yellow-green
GRR169	Santa Rita Peak, San Benito Co., CA, U.S.A.	serpentinite	andradite	yellow-green
GRR684	San Benito Co., CA, U.S.A.	serpentinite	melanite	black
GRR1263	San Benito Co., CA, U.S.A.	serpentinite	melanite	black
GRR1328	San Benito Co., CA, U.S.A.	serpentinite	melanite	black
GRR1765	Ural Mtns, Russia	serpentinite	demantoid	green
GA32	Davib Ost, South Africa	skarn	andradite	yellow-green
GA35	Grua, Norway	skarn	andradite	yellow-brown
GRR54	Stanley Butte, Graham Co., AZ, U.S.A.	skarn	andradite	yellow
GRR149	Franklin, NJ, U.S.A.	skarn	andradite	orange-brown
GRR1015	Franklin, NJ, U.S.A.	skarn	andradite	yellow-orange
GRR1137a2	Stanley Butte, Graham Co., AZ, U.S.A.	skarn	andradite	brown-yellow
GRR1447	Humbolt Co., NV, U.S.A.	skarn	andradite	yellow-brown
GRR1448	Reeseville, NY, U.S.A.	skarn	andradite	orange-brown
GA24	Kaiserstuhl, Germany	phonolite	melanite	black
GA36	Frascati, Italy	magmatic	melanite	black
GRR1446	Frascati, Italy	magmatic	melanite	black
CITH3110	Rusinga Island, Kenya	magmatic	melanite	black
GAIV/1/4	375 °C, 1.5 kbar, HM††	synthetic powder	hydroandradite	pale red
GAIIIa/3	375 °C, 1.5 kbar, HM††	synthetic powder	hydroandradite	pale green

* Quantitative amounts of OH^- in andradite garnets are determined from the grossular calibration of Rossman and Aines (1991).
† From Wise and Moller (1990).
‡ Rim.
§ From Amthauer et al. (1979).
‖ Inhomogenous.
Compositionally zoned.
** Described in Kühberger et al. (1989).
†† HM = Fe_2O_3/Fe_3O_4-oxygen fugacity buffer.
‡‡ Composition from XRD parameters.

was chosen for most samples with 1000 scans suitable to produce high-quality spectra. Reference spectra were taken in air. In addition, some reflectance spectra from synthetic garnet powders were taken with the same experimental setup using polished Au as a reference. Comparison of single-crystal spectra and reflectance spectra of the same garnet sample revealed a similar resolution of the OH features in each case.

Because an independent calibration of the OH^- concentration in andradite does not exist, the calibration of Rossman and Aines (1991) for grossular was used to estimate the H content of andradite. The integrated absorbance under the OH^- stretching region of the IR spectrum (normalized to a 1 cm thick sample) is determined and the H content is obtained by reference to the grossular calibration.

Chemical analyses of the samples were performed with an automated JEOL 733 electron microprobe using a 15 nA beam current. Data were corrected using the program CITZAF (Armstrong 1988) employing the absorption correction of Armstrong (1982), the atomic number correction of Love et al. (1978), and the fluorescence correction of Reed (1965) as modified by Armstrong (1988). The structural formulae of the samples normalized to 12 O atoms are reported in Table 1.

Andradite-hydroandradite solid solutions were synthesized hydrothermally from glass of an appropriate composition at temperatures between 300 and 400 °C, pressures of 1.5 and 2.0 kbar, and the oxygen fugacities of the hematite + magnetite buffer (Tippelt and Amthauer, in preparation). Purity and homogeneity of the samples were checked by XRD of powders using Cu$K\alpha$-radiation. The chemical composition, in particular the OH^- content, X was calculated from the lattice constant a_o according to the regression equation of Huckenholz and Fehr (1982)

$$a_o = 12.057 + 0.4906\ X + 0.2379\ X^2 - 0.0824\ X^3.$$

The small grain sizes (<20 μm) and morphology of the synthetic samples made it impractical to obtain spectra from single crystals; therefore only powder spectra were taken of the synthetic garnet.

RESULTS

The IR spectra of three andradite samples from serpentinites are shown in Figure 1. GRR134 is representative of almost pure andradite and exhibits the simplest spectrum, i.e., a dominant absorption band at 3555 cm^{-1}. Weak higher energy absorptions and a weak shoulder on the low energy site of the main peak are also present. The IR spectrum of andradite from the Ural mountains (GRR1765) looks almost identical. This garnet is also almost pure end-member andradite with minor amounts of Mg (0.01 wt%), Al (0.01 wt%), and Cr (0.05 wt%). Both are clear and contain 0.10 wt% H_2O. The spectrum of the San Benito andradite (GRR1263) is more complex. Although the overall intensity is lower (0.01 wt% H_2O), it

TABLE 1—*Continued*

	Formula proportions			wt%H_2O*
GRR1669	$(Ca_{3.00}Mg_{0.04})$	$[Fe^{3+}_{1.80}Al_{0.20}]$	$Al_{0.05}Si_{2.74}O_{12}$	5.92†
GA33	$(Ca_{2.98}Mg_{0.01}Mn_{0.01})$	$[Fe^{3+}_{2.01}Al_{0.003}Ga_{0.001}]$	$Si_{2.99}O_{12}$	<0.01
GA34	$(Ca_{2.99}Mg_{0.01})$	$[Fe^{3+}_{2.01}V_{0.001}Ti_{0.001}]$	$Fe^{3+}_{0.02}Si_{2.98}O_{12}$	0.07
GRR48 rim	$(Ca_{3.03}Mg_{0.01})$	$[Fe^{3+}_{1.98}]$	$Si_{2.97}O_{12}$	0.10‡
GRR134	$(Ca_{2.97}Mg_{0.02}Mn_{0.002})$	$[Fe^{3+}_{2.01}Al_{0.01}Cr_{0.001}V_{0.001}Ga_{0.003}Ti_{0.002}]$	$P_{0.001}Si_{2.99}O_{12}$	0.09
GRR169	$(Ca_{3.00}Mg_{0.02}Fe^{2+}_{0.02})$	$[Fe^{3+}_{1.86}Al_{0.05}Ti_{0.02}]$	$Si_{3.03}O_{12}$	0.15
GRR684	$(Ca_{3.02}Mg_{0.01}Mn_{0.01}Fe^{2+}_{0.02})$	$[Fe^{3+}_{1.98}Al_{0.02}Ti_{0.02}]$	$Si_{2.92}O_{12}$	1.17
GRR1263	not analyzed			0.04
GRR1328	$(Ca_{2.99}Mg_{0.07})$	$[Fe^{3+}_{1.62}Al_{0.16}Ti_{0.13}]$	$Si_{2.77}O_{12}$	2.45
GRR1765	$(Ca_{2.99}Mg_{0.01}Mn_{0.001})$	$[Fe^{3+}_{1.94}Cr_{0.07}V_{0.001}Ga_{0.001}Ti_{0.003}Zr_{0.001}]$	$P_{0.001}Si_{2.99}O_{12}$	0.10
GA32	$(Ca_{2.98}Mg_{0.002}Mn_{0.01}Fe^{2+}_{0.01})$	$[Fe^{3+}_{1.99}Ti_{0.001}Sn_{0.011}]$	$Fe^{3+}_{0.02}Si_{2.98}O_{12}$	0.15§
GA35	$(Ca_{2.95}Mg_{0.01}Mn_{0.04})$	$[Fe^{3+}_{1.73}Al_{0.24}Cr_{0.001}Ti_{0.03}]$	$Al_{0.03}Si_{2.97}O_{12}$	0.05
GRR54	$(Ca_{3.06}Mg_{0.01}Mn_{0.01})$	$[Fe^{3+}_{1.94}Al_{0.03}]$	$Si_{2.95}O_{12}$	0.38
GRR149	$(Ca_{2.72}Mg_{0.01}Mn_{0.67}Fe^{2+}_{0.20})$	$[Fe^{3+}_{1.24}Al_{0.46}Ti_{0.02}]$	$Si_{3.14}O_{12}$	0.04
GRR1015	$(Ca_{2.29}Mn_{0.71}Fe^{2+}_{0.03})$	$[Fe^{3+}_{1.47}Al_{0.46}Ti_{0.01}]$	$Si_{3.03}O_{12}$	1.44‖
GRR1137a2	$(Ca_{2.98}Mg_{0.01}Mn_{0.02}Fe^{2+}_{0.01})$	$[Fe^{3+}_{1.84}Al_{0.14}]$	$Si_{3.02}O_{12}$	0.40#
GRR1447	$(Ca_{2.41}Mg_{0.01}Mn_{0.59}Fe^{2+}_{0.05})$	$[Fe^{3+}_{1.52}Al_{0.36}Ti_{0.03}]$	$Si_{3.04}O_{12}$	0.03
GRR1448	$(Ca_{2.96}Mg_{0.01}Mn_{0.01}Fe^{2+}_{0.06})$	$[Fe^{3+}_{1.74}Al_{0.19}]$	$Si_{2.96}O_{12}$	<0.01
GA24	$(Ca_{2.89}Mg_{0.06}Fe^{2+}_{0.04})$	$[Fe^{3+}_{0.88}Fe^{2+}_{0.07}Al_{0.23}Ti_{0.74}Mg_{0.05}Mn_{0.03}]$	$Si_{2.47}Fe^{3+}_{0.32}Fe^{2+}_{0.13}Ti_{0.08}O_{12}$	0.01**
GA36	$(Ca_{2.88}Mg_{0.07}Mn_{0.02})$	$[Fe^{3+}_{1.30}Al_{0.50}V_{0.01}Ga_{0.002}Ti_{0.18}Zr_{0.01}]$	$P_{0.001}Al_{0.15}Si_{2.85}O_{12}$	0.03
GRR1446	$(Ca_{2.92}Mg_{0.06}Mn_{0.02}Fe^{2+}_{0.08})$	$[Fe^{3+}_{1.21}Al_{0.65}Ti_{0.13}]$	$Si_{2.95}O_{12}$	0.04
CITH3110	$(Ca_{2.89}Mg_{0.11}Mn_{0.02}Fe^{2+}_{0.26})$	$[Fe^{3+}_{1.17}Al_{0.10}Ti_{0.88}]$	$Si_{2.51}O_{12}$	0.02
GAIV/1/4	Ca_3	$Fe^{3+}_{2.0}$	$(SiO_4)_{2.81}(H_4O_4)_{0.19}$‡‡	
GAIIIa/3	Ca_3	$Fe^{3+}_{2.0}$	$(SiO_4)_{2.71}(H_4O_4)_{0.29}$‡‡	

exhibits distinct peaks at the high energy side of the main peak where the other two showed only weak absorptions. Even though this particular sample was lost before it could be chemically analyzed, it can be concluded by comparison with the chemical composition of other andradites from San Benito (Table 1) that its chemical diversity and complexity is greater than those of the other two andradite samples illustrated in Figure 1.

The IR spectrum of an andradite occurring with zeolites and julgoldite, $Ca_2Fe^{2+}(Fe^{3+},Al_2)(SiO_4)(Si_2O_7)(OH)_2 \cdot H_2O$, in vugs in a basalt near Bombay, India, is displayed in Figure 2. This garnet, which formed at about 200 °C at 500 bars (Wise and Moller 1990), has a high OH content equivalent to 5.92 wt% H_2O. Its spectrum exhibits a prominent absorption band near 3560 cm^{-1} and a second higher energy band at 3610 cm^{-1}. Two prominant bands are also found in the spectrum of natural hydrogrossular with low Si content, i.e., Si = 1.64 (Rossman and Aines 1991), also plotted in Figure 2. The spectra are scaled for comparable band heights. Even though the absorption bands of the hydroandradite are shifted to lower energies in comparison to hydrogrossular, an analogous substitution mechanism is suggested by these similarities. The very weak, broad absorption between 3400 and 3350 cm^{-1} may be assigned to nonstructural H_2O.

The spectrum of the hydroandradite synthesized at 375 °C and 1.5 kbar (GAIV1/4) exhibits an intense absorption band with its maximum at 3560 cm^{-1}, a slightly less intense sharp band at 3610 cm^{-1}, some unresolved shoulders at high energy, and a broad shoulder at the low energy most probably resulting from nonstructural H_2O (Fig. 2). The shape of the spectrum is similar to the spectra of the hydrogrossular and the natural hydroandradite in Figure 2. The two peaks indicates two different mechanisms for the substitution of Si by OH^-. The peak maxima have the same energies as those in the natural hydroandratite spectrum. The spectrum in the OH^- region of the synthetic andradite reported by Armbruster and Geiger has its main peak at essentially the same position as GAIV1/4, but has its second component at lower energy, unlike GAIV1/4, which has its second component at higher energy. The reason for this difference is not known. We also note that the most intense peak at 3555 cm^{-1} in the spectrum of the Val Malenco andradite occurs close to the same wavenumber as the strongest absorption band in the spectra of natural and synthetic hydroandradites.

The IR spectrum of melanite from Rusinga Island (Fig. 3) shows two main peaks of low intensity near 3530 and 3560 cm^{-1} superimposed on the low energy flank of a strong absorption in the NIR, which is most probably due to Fe^{2+} in the tetrahedral sites of the garnet. The spectrum is representative of the low OH^- content garnets (0.02 wt% H_2O) from volcanic environments such as the melanites from Kaiserstuhl and Magnet Cove, whose spectra show many similarities.

The IR spectrum (Fig. 4) of an andradite from Stanley Butte, Arizona, (GRR1137) with 0.40 wt% H_2O is representative of andradite from skarns. It exhibits a higher degree of complexity, i.e., four resolved peaks between 3550 and 3630 cm^{-1} and three shoulders at higher energies between 3630 and 3700 cm^{-1}.

Five spectra of different zones of a melanite from Santa Rita Peak, San Benito County, California, are displayed in Figure 5. This melanite formed at similar *P-T* conditions as the andradite from the same occurrence

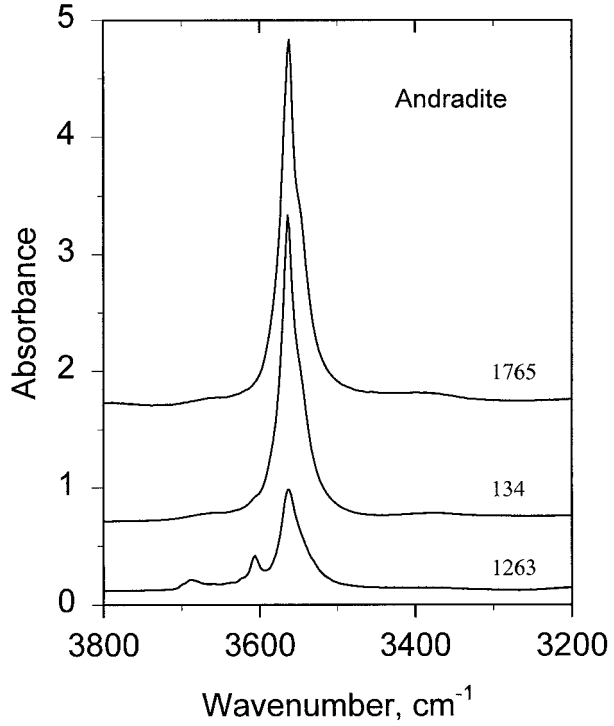

FIGURE 1. Comparison of the IR spectra of natural andradites from serpentinites. From top to bottom: Ural mountains, USSR (GRR1765); Val Malenco, Italy (GRR134); San Benito County, California (GRR1263). The spectra are plotted for 1 mm crystal thickness.

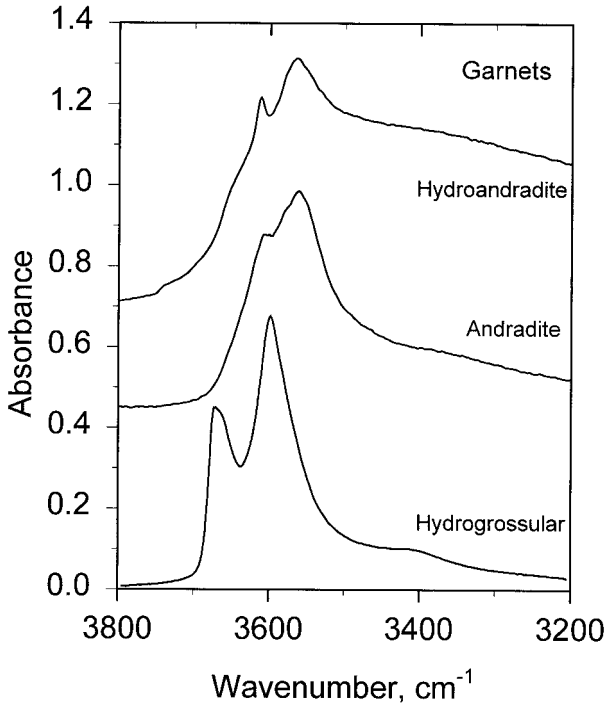

FIGURE 2. Comparison of the IR spectra of hydrogrossular from Crestmore, California, $Ca_3Al_2[(SiO_4)_{1.64}(O_4H_4)_{1.36}]$ (Rossman and Aines 1991); hydrous andradite from Bombay, India (GRR1669); synthetic hydroandradite $Ca_3Fe_2^{3+}[(SiO_4)_{2.81}(O_4H_4)_{0.19}]$ (GAIV1/4). The spectra are scaled for comparable band heights, i.e., 4.2 μm thickness (Crestmore); 10.5 μm thickness (Bombay); and powdered synthetic hydroandradite.

(GRR1263 in Fig. 1). The spectra show an increasing number of resolved peaks and shoulders going from the dominantly yellow-green rim to the core with dark amber-brown, almost ''black'' colors. The quantitative evaluation of the spectra (see below) indicates a higher OH^- content in the dark regions.

The OH^- contents (as H_2O) are determined from the integral absorbance (Table 1). Most samples are heterogeneous. Variability as large as a factor of two is common. The tabulated values represent averages of several spectra taken from different points on a given sample. In almost pure end-member andradite and other yellow-green andradite from serpentinites, the amount of OH^- is small (<0.01 to 0.15 wt% H_2O). As their Ti-content increases and they become deeply colored melanite, their OH^- content increases up to about 2.5 wt% H_2O. The OH^- contents of skarn andradite vary between <0.01 and 1.44 wt% H_2O. The OH^- contents of melanite of volcanic origin are generally the lowest (0.01 to 0.04 wt% H_2O). The highest amount of OH^- we measured is in the hydroandratite from a cavity in a basalt, which obviously is a post magmatic, low-temperature formation. It should be emphasized that all the andradite we have studied contained OH^-.

DISCUSSION

Comparison of our spectra with those from similar studies on other natural and synthetic garnets (e.g., Aines and Rossman 1985; Rossman and Aines 1991) shows that H enters the andradite structure in the form of structurally bonded OH^-. The similarities to the IR spectra of natural and synthetic hydrogrossular shown in Figure 2 suggest that the substitution $SiO_4^{4-} \leftrightarrow (O_4H_4)^{4-}$ is important in andradite. The two absorption maxima in the spectra in Figure 2 are explained either by two slightly different substitution mechanisms in the tetrahedron or by different nearest neighbors of $(O_4H_4)^{4-}$, such as $(SiO_4)^{4-}$ or $(O_4H_4)^{4-}$, respectively (Rossman and Aines 1991). The lower energies of the two maxima in andradite may be related to greater average tetrahedral cation-anion distances in andradite compared to grossular. The absorption peak in the spectra of the andradite from Val Malenco and the Ural Mountains occurs at almost the same energy as the most intense peak in the spectra of the natural and synthetic hydroandradite and therefore may also represent the hydrogarnet substitution. Also, the most intense peak near 3560 cm^{-1} in the spectrum of Figure 3 may be assigned to the hydrogarnet substitution. Locock et al. (1995) report an absorption band at almost the same energy (3564 cm^{-1}) in the spectrum of a schorlomite. Diffraction studies (Lager et al. 1989; Armbruster 1995) confirm the importance of the hydrogarnet substitution in andradite as well as melanite.

Despite one additional peak at about 3530 cm^{-1}, the

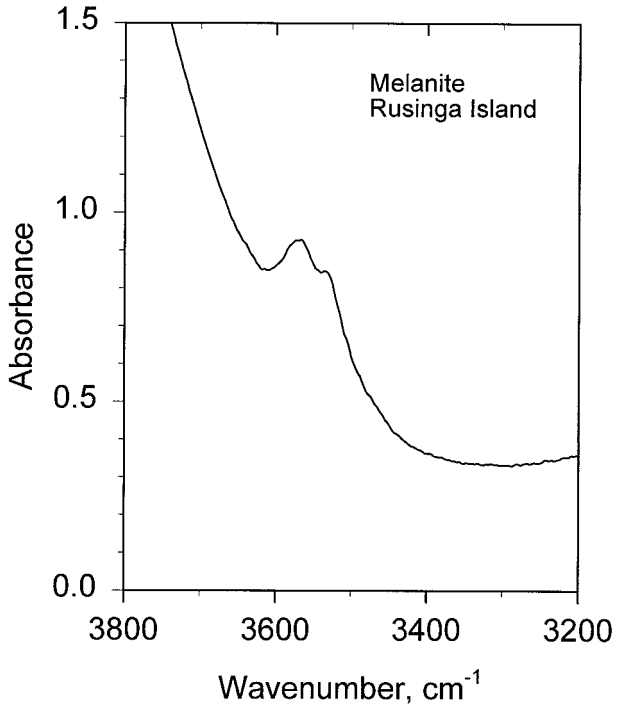

FIGURE 3. IR spectrum of andradite (CITH3110) from Rusinga Island, Kenya, is representative of the low OH^- content garnets from volcanic environments. The increasing absorbance toward the left is from Fe^{2+} in the tetrahedral site of the garnet structure. The spectrum is scaled for 1 mm crystal thickness.

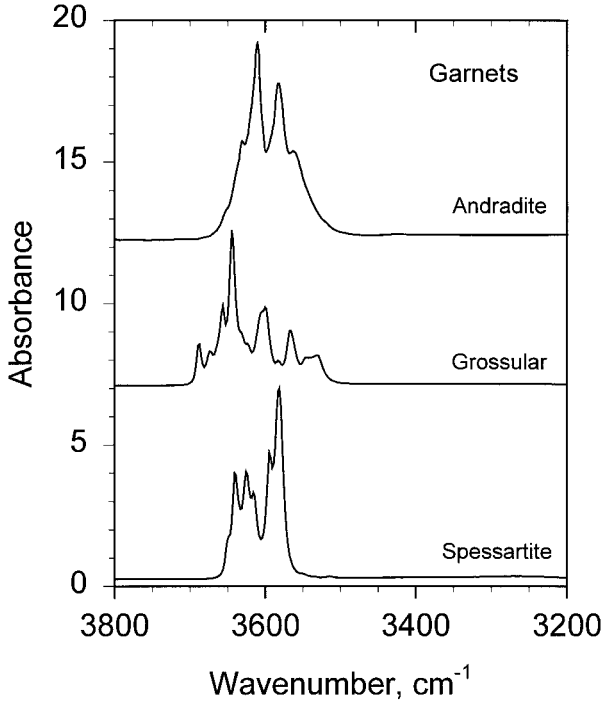

FIGURE 4. Comparison of the IR spectra of Stanley Butte andradite (GRR1137, scaled for 1.0 mm), grossular (GRR771, Meralini Hills, Tanzania, scaled for 1.2 mm), and spessartite (GRR43-1, Rutherford no. 2 Mine, Virginia, U.S.A., scaled for 0.7 mm). The spectra of all these garnets exhibit several absorption bands that document multi-site substitution of OH^-.

spectra of samples of melanite in this study are relatively simple in comparison with most of the other IR spectra of the samples of this study. The complexity of the andradite spectra is seen in the spectra of many other kinds of natural garnets. For comparison, the spectra of a grossular and a spessartite are displayed in Figure 4. Their spectra reveal more absorption bands than those that may be due to the hydrogarnet substitution. Thus, most garnets, including andradite, have other kinds of incorporation of OH^- than just the substitution $(SiO_4)^{4-} \leftrightarrow (O_4H_4)^{4-}$ (Rossman and Aines 1991). Unfortunately, a definite assignment to lattice positions does not exist. Incorporation of OH^- at the octahedral sites or even at the dodecahedral sites as a coupled substitution with ions of transition metals such as Fe is possible.

The reasons for the higher degree of complexity in some spectra are not obvious. Temperature of formation cannot be the only deciding factor for a high degree of multi-site OH^- substitution. Skarn andradite forms at higher temperatures than the garnet from serpentinites and their spectra show more resolved absorption features than the garnet from serpentinites. However, melanite from volcanic rock with low amounts of H_2O formed at even higher temperatures than the skarn andradite, but its spectra are comparatively simple. Also, high OH^- content cannot be the only reason for a higher degree of complexity in the spectra, because the hydroandradite occurring in a cavity in a basalt has the highest H_2O content of all the garnets of this study, yet its spectrum exhibits just the two absorption bands that are also observed in the spectra of the synthetic hydroandradite. On the other hand, the zoned melanite from San Benito (Fig. 5) shows increasing complexity in its spectrum moving from the yellow-brown rim to the deep brown-amber core. From other investigations on Ti-rich garnet, it is known that these darker areas have higher amounts of Ti and a slight Si deficiency. In Si deficient garnets, Ti, Fe, and Al are distributed over octahedral and tetrahedral sites. At low oxygen fugacities they may contain even Fe^{2+} (Kühberger et al. 1989). Therefore, their crystal chemistry is more complex and they have more and different kinds of defects. That is why the possibilities for the incorporation of OH^- increase, partially for the achievement of local sample balance. This multi-site OH^- substitution causes a higher degree of complexity in the IR spectra. Similarly, the skarn andradites are often zoned and may have a complex crystal chemistry. Therefore, one reason for an increased number of absorption features in their spectra is a greater complexity of the crystal chemistry.

In their experimental study, Huckenholz and Fehr (1982) have shown that the incorporation of hydroandradite, $Ca_3Fe_2(OH)_{12}$, in andradite, $Ca_3Fe_2Si_3O_{12}$, decreases distinctly with elevated temperature and less dis-

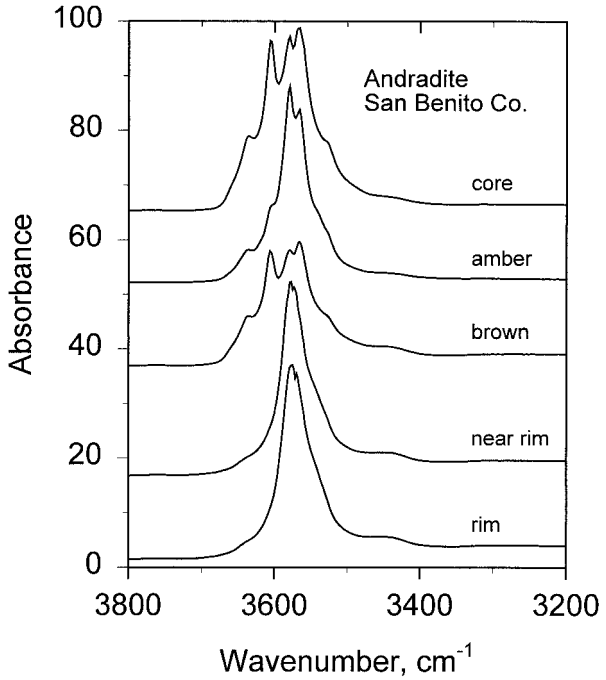

FIGURE 5. Zonation in melanite garnet from Santa Rita Peak, San Benito County, California (GRR1263). The IR spectrum is more complex in the darker regions where the OH^- content is higher. The spectra are scaled for 1 mm crystal thickness.

tinctly with increasing pressure. Our results generally agree. The andradite (GRR1669) from a cavity in a basalt with nearly 6 wt% H_2O represents a low-temperature, low-pressure postmagmatic formation. The melanite from volcanic rocks formed at much higher temperatures and are characterized by low amounts of H_2O (0.01–0.04 wt%). Andradite from skarns or melanite from veins in serpentinites have amounts of H_2O between those extremes.

ACKNOWLEDGMENTS

The authors thank G. Tippelt (Salzburg) for the hydroandradite synthesis and S. Ebner for typing the manuscript. We thank the Fulbright Commission and the Fonds zur Förderung der wissenschaftlichen Forschung in Vienna for financial support of GA through grant P10010GEO during his stay in Pasadena, and the National Science Foundation (U.S.A.) for support through grant no. EAR-9218980.

REFERENCES CITED

Aines, R.D. and Rossman, G.R. (1985) The hydrous component in garnets: pyralspites. American Mineralogist, 69, 1116–1126.

Amthauer, G., McIver, J.R., and Viljoen, E.A. (1979) ^{57}Fe and ^{119}Sn Mössbauer studies of natural tin-bearing garnets. Physics and Chemistry of Minerals, 4, 235–244.

Armbruster, T. (1995) Structure refinement of hydrous andradite, $Ca_3Fe_{1.54}Mn_{0.20}Al_{0.26}(SiO_4)_{1.65}(O_4H_4)_{1.35}$, from the Wessels mine, Kalahari manganese field, South Africa. European Journal of Mineralogy, 7, 1221–1225.

Armbruster, T. and Geiger, C.A. (1993) Andradite crystal chemistry, dynamic X-site disorder and structural strain in silicate garnets. European Journal of Mineralogy, 5, 59–71.

Armstrong, J.T. (1982) New ZAF and α-factor correction procedures for the quantitative analysis of individual microparticles. In K.F.J. Heinrich, Ed., Microbeam Analysis, p. 175–180. San Francisco Press, San Francisco.

———(1988) Quantitative analysis of silicate and oxide materials: Comparison of Monte Carlo, ZAF, and Φ(ρz)procedures. In D.E. Newbury, Ed., Microbeam Analysis, p. 239–246. San Francisco Press, San Francisco.

Flint, E., McMurdie, H.F., and Wells, L.S. (1941) Hydrothermal and X-ray studies of the garnet-hydrogarnet series and the relationship of the series to hydration products of portland cement. Journal of Research of the National Bureau of Standards, 26, 13–33.

Gustafson, W.J. (1974) The stability of andradite, hedenbergite, and related minerals in the system Ca-Fe-Si-O-H. Journal of Petrology, 15, 455–496.

Huckenholz, H.G. and Fehr, K.T. (1982) Stability relationship of grossular + quartz + wollastonite + anorthite II. The effect of grandite-hydrograndite solid solution. Neus Jahrbuch der Mineralogie Abhandlungen, 145, 1–33.

Kobayashi, S. and Shoji, T (1987) Infrared spectra and cell dimensions of hydrothermally synthesized grandite-hydrograndite series. Mineralogical Journal, 13, 490–499.

Kühberger, A., Fehr, K.T., Huckenholz, H.G., and Amthauer, G. (1989) Crystal chemistry of a natural schorlomite and Ti-andradites synthesized at different oxygen fugacities. Physics and Chemistry of Minerals, 16, 734–740.

Lager, G.A., Armbruster, T., Rotella, F.J., and Rossman, G.R. (1989) OH substitution in garnets: X-ray and neutron diffraction, infrared, and geometric-modeling studies. American Mineralogist, 74, 840–851.

Locock, A., Luth, R.W., Cavell, G.G., Smith, D.G.S., and Duke, M.J.M. (1995) Spectroscopy of the cation distribution in the schorlomite species of garnet. American Mineralogist, 80, 27–38.

Love, G., Cox, M.G., and Scott, V.D. (1978) A versatile atomic number correction for electron-probe microanalysis. Journal of Physics D, 11, 7–27.

Macke de Lummen, G.V. (1986) Fluor-bearing hydro-andradite from an altered basalt in the Land's End area, SW England. Bulletin de Minèralogie, 109, 613–616.

Onuki, H., Akasaka, M., Yoshida, T., and Nedachi, M. (1982) Ti-rich hydroandradites from the Sanbagawa metamorphic rocks of the Shibukawa area, central Japan. Contributions to Mineralogy and Petrology, 80, 183–188.

Peters, T. (1965) A water-bearing andradite from the Totalp serpentine (Davos, Switzerland). American Mineralogist, 50, 1482–1486.

Reed, S.J.B. (1965) Characteristic fluorescence correction in electron-probe microanalysis. British Journal of Applied Physics, 16, 913–926.

Rossman, G.R. and Aines, R.D. (1991) The hydrous components in garnets: Grossular-hydrogrossular. American Mineralogist, 76, 1153–1164.

Suwa, Y., Tamai, Y., and Naka, S. (1976) Stability of synthetic andradite at atmospheric pressure. American Mineralogist, 61, 26–28.

Wise, W.S. and Moller, W.M. (1990) Occurrence of Ca-Fe silicate minerals with zeolites in basalt cavities at Bombay, Indian. European Journal of Mineralogy, 2, 875–883.

MANUSCRIPT RECEIVED AUGUST 1, 1996
MANUSCRIPT ACCEPTED FEBRUARY 4, 1998
PAPER HANDLED BY ANNE M. HOFMEISTER